

Oncogenic transcription factor *Evi1* regulates hematopoietic stem cell proliferation through *GATA-2* expression

Hiromi Yuasa^{1,7}, Yuichi Oike^{1,7,*},
Atsushi Iwama², Ichiro Nishikata³,
Daisuke Sugiyama⁴, Archibald Perkins⁵,
Michael L Mucenski⁶, Toshio Suda^{1,*}
and Kazuhiro Morishita^{3,*}

¹Department of Cell Differentiation, The Sakaguchi Laboratory, School of Medicine, Keio University, Tokyo, Japan, ²Department of Cellular and Molecular Biology, Graduate School of Medicine, Chiba University, Chiba, Japan, ³Department of Biochemistry, Medical College, University of Miyazaki, Miyazaki, Japan, ⁴Division of Cellular Therapy, Advanced Clinical Research Center, Institute of Medical Science, University of Tokyo, Tokyo, Japan, ⁵Department of Pathology, Yale University School of Medicine, New Haven, CT, USA and ⁶Division of Pulmonary Biology, Cincinnati Children's Hospital Medical Center, Cincinnati, OH, USA

The ecotropic viral integration site-1 (*Evi1*) is an oncogenic transcription factor in murine and human myeloid leukemia. We herein show that *Evi1* is predominantly expressed in hematopoietic stem cells (HSCs) in embryos and adult bone marrows, suggesting a physiological role of *Evi1* in HSCs. We therefore investigate the role and authentic target genes of *Evi1* in hematopoiesis using *Evi1*^{-/-} mice, which die at embryonic day 10.5. HSCs in *Evi1*^{-/-} embryos are markedly decreased in numbers *in vivo* with defective self-renewing proliferation and repopulating capacity. Notably, expression rate of *GATA-2* mRNA, which is essential for proliferation of definitive HSCs, is profoundly reduced in HSCs of *Evi1*^{-/-} embryos. Restoration of the *Evi1* or *GATA-2* expression in *Evi1*^{-/-} HSCs could prevent the failure of *in vitro* maintenance and proliferation of HSC through upregulation of *GATA-2* expression. An analysis of the *GATA-2* promoter region revealed that *Evi1* directly binds to *GATA-2* promoter as an enhancer. Our results reveal that *GATA-2* is presumably one of critical targets for *Evi1* and that transcription factors regulate the HSC pool hierarchically.

The EMBO Journal (2005) 24, 1976–1987. doi:10.1038/sj.emboj.7600679; Published online 12 May 2005

Subject Categories: chromatin & transcription; development

Keywords: angiopoiesis; *Evi1*; *GATA-2*; hematopoiesis

*Corresponding authors. Y Oike, T Suda, Department of Cell Differentiation, The Sakaguchi Laboratory, School of Medicine, Keio University, Tokyo, Japan. Tel.: +81 3 5363 3475; Fax: +81 3 5363 3474; E-mails: oike@sc.itc.keio.ac.jp or sudato@sc.itc.keio.ac.jp or K Morishita, Department of Biochemistry, Faculty of Medicine, Miyazaki Medical College, University of Miyazaki, 5200 Kihara, Miyazaki 889-1692, Japan. Tel.: +81 3 5363 3473; Fax: +81 3 5363 3474; E-mail: kmorishi@med.miyazaki-u.ac.jp
⁷These authors contributed equally to this work

Received: 19 July 2004; accepted: 21 April 2005; published online: 12 May 2005

Introduction

The ecotropic viral integration site-1 (*Evi1*) was first identified as a common site of retroviral integration in murine myeloid tumors (Morishita *et al*, 1988; Mucenski *et al*, 1988). Rearrangements involving human *Evi1* on chromosome 3q26 often activate its expression in human acute myeloid leukemia (AML) and myelodysplastic syndrome (MDS) (Morishita *et al*, 1992b; Mitani *et al*, 1994). *Evi1* is a member of the SET/PR domain family of zinc-finger transcription factors and it contains two separated zinc-finger DNA-binding domains, which recognize different DNA sequences (Matsugi *et al*, 1990; Morishita *et al*, 1995). However, the authentic target genes of *Evi1* have not yet been identified.

The expression of *Evi1* in adult mice is restricted to the kidney and ovary (Morishita *et al*, 1990), whereas *Evi1* is expressed abundantly in several embryonic tissues in the developing mouse (Perkins *et al*, 1991), suggesting that *Evi1* plays a role in normal development. In fact, mice lacking *Evi1* tend to exhibit widespread hypocoellularity, hemorrhaging and a disruption of the paraxial mesenchyme and, as a result, they die at approximately 10.5 days postcoitus (d.p.c.; E10.5). In addition, homozygous embryos show defects in the heart, somites, cranial ganglia and the peripheral nervous system (Hoyt *et al*, 1997). These findings indicate that *Evi1* plays an important role in cell proliferation and/or differentiation in a variety of cell types. Moreover, *Evi1* has been shown to be expressed in bone marrow hematopoietic stem cells (HSCs), implying that *Evi1* plays a role in the regulation of HSCs (Phillips *et al*, 2000; Park *et al*, 2002; Shimizu *et al*, 2002). On the other hand, no detailed expression profiles of *Evi1* or its physiological roles in primary hematopoietic cells have yet been published. As a result, we attempted to clarify the role of *Evi1* in the development of HSCs during embryonic hematopoiesis.

In this study, we performed a detailed analysis of hematopoiesis in mice lacking *Evi1* and found that the development and expansion of definitive HSCs is severely impaired in homozygous (*Evi1*^{-/-}) embryos. This hematological phenotype is reminiscent of that observed in *GATA-2*-deficient embryos. The expression of *Evi1* or *GATA-2* in HSCs from *Evi1*^{-/-} embryos could prevent the failure of *in vitro* development and the proliferation of HSCs through an upregulation of *GATA-2* expression. Since the *GATA-2* mRNA levels in *Evi1*^{-/-} embryos decreased markedly, we localized the *cis*-element to the *GATA-2* promoter region through which *Evi1* directly regulates *GATA-2* transcription *in vitro*. Our data provide the first evidence demonstrating that *Evi1* plays a physiological role in normal hematopoiesis, while also identifying *Evi1* as a transcriptional regulator epistatic to *GATA-2*, which controls both HSC maintenance and proliferation.

Results

Evi1 expression in embryonic and adult hematopoietic stem cells

We first examined the expression pattern of *Evi1* mRNA in various hematopoietic lineage cells. Quantitative RT-PCR revealed that *Evi1* mRNA is predominantly expressed in both the embryonic and adult HSC fractions, that is, CD34⁺CD45⁺c-Kit⁺ cells from mouse embryos and c-Kit⁺Sca-1⁺Lin⁻ cells from adult mouse bone marrow, respectively (Figure 1A). In addition, we found an abundant *Evi1* expression in both the yolk sac and para-aortic splanchnopleural (P-Sp) region, where primitive (embryo-type) and definitive (adult-type) hematopoiesis occurs, respectively (Godin *et al*, 1995). These findings led to a detailed analysis aimed at determining the role of *Evi1* in normal hematopoiesis by analyzing *Evi1* homozygous mutant mice.

In this study, we analyzed 126 wild-type, 264 heterozygous (*Evi1*^{+/-}) and 124 homozygous (*Evi1*^{-/-}) embryos at E9.5, which together demonstrated a proportion of 1:2:1 in keeping with Mendel's first law. By E11.0, all homozygous *Evi1*^{-/-} embryos were dead, but living embryos could still be recovered at E9.5. The yolk sac at E9.5 of *Evi1*^{-/-} embryos was paler than those of wild-type and heterozygous *Evi1*^{+/-} embryos (Figure 1Ba-c). Although the total number of blood cells from the yolk sac decreased to 20% of that in the littermates in *Evi1*^{-/-} embryos (Supplementary Figure 1A), ϵ and β hemoglobin staining revealed no maturational defect of primitive erythroid cells in the yolk sac (data not shown). In addition, yolk sac cells from *Evi1*^{-/-} embryos showed no alteration in the erythroid and granulocyte-macrophage (GM) colony formation in comparison to the wild-type counterparts (Supplementary Figure 1B). Since *Evi1*^{-/-} embryos exhibited pericardial effusion with hemorrhaging (Figure 1Bd-f), the reduction in yolk sac erythrocytes is probably due to a loss of blood cells. At E9.5, the body of *Evi1*^{-/-} embryos was smaller than that of the wild-type littermates, but the 'turning' of the embryos with 21-29 pairs of somites had finished, suggesting that they had developed normally.

Decreased *in vitro* proliferation of hematopoietic stem cells in *Evi1*^{-/-} mutants

We next determined the capacity for definitive hematopoiesis, which occurs in the P-Sp region at E9.5. Although the recovered number of cells from the P-Sp region of *Evi1*^{+/+}, *Evi1*^{+/-} and *Evi1*^{-/-} embryos was almost equal among the three lineages (Supplementary Table 1), the number of CD45⁺ hematopoietic cells dramatically decreased in the P-Sp region from the *Evi1*^{-/-} embryos, in comparison to that from *Evi1*^{+/-} or wild-type *Evi1*^{+/+} (Figure 2Aa). Accordingly, the P-Sp region of *Evi1*^{-/-} embryos contained significantly fewer CD34⁺c-Kit⁺CD45⁺ HSCs than in the controls, although the percentages of HSCs in CD45⁺ cells showed almost the same levels (70-80%) for the *Evi1*^{+/+}, *Evi1*^{+/-} and *Evi1*^{-/-} embryos (Figure 2Ab and c). These findings suggest that *Evi1* possibly plays a role in the development and/or expansion of HSCs.

We next examined the capacity of HSCs from *Evi1*^{-/-} embryos to proliferate using an *in vitro* P-Sp explant/OP9 stromal cell coculture system (Takakura *et al*, 2000). After P-Sp explants were cultured on OP9 cells for 7 days, fractions of

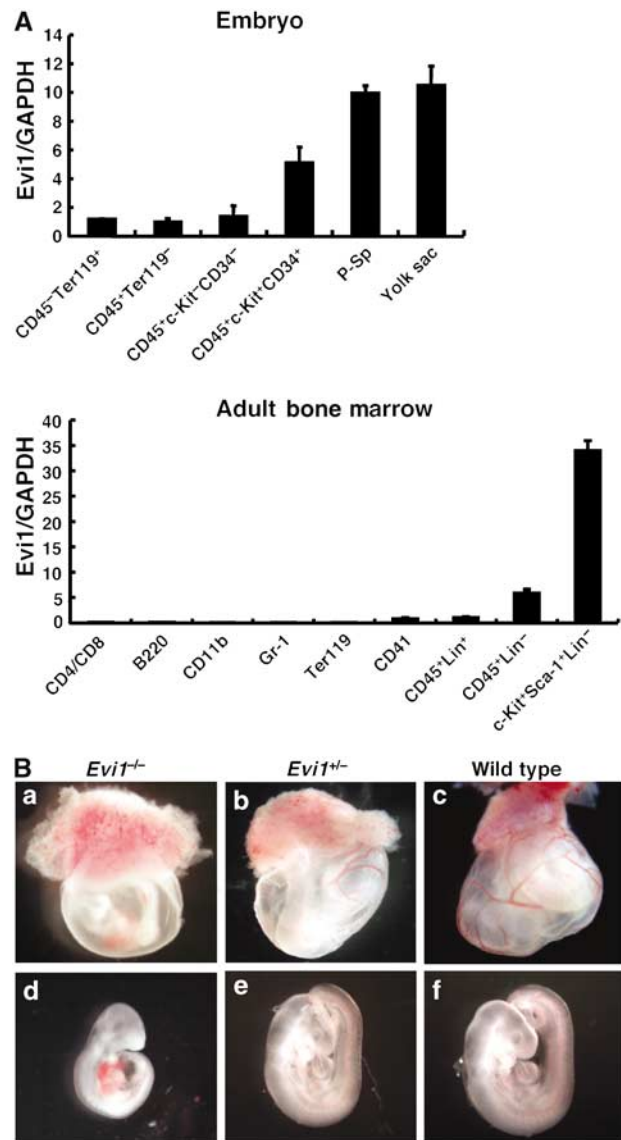
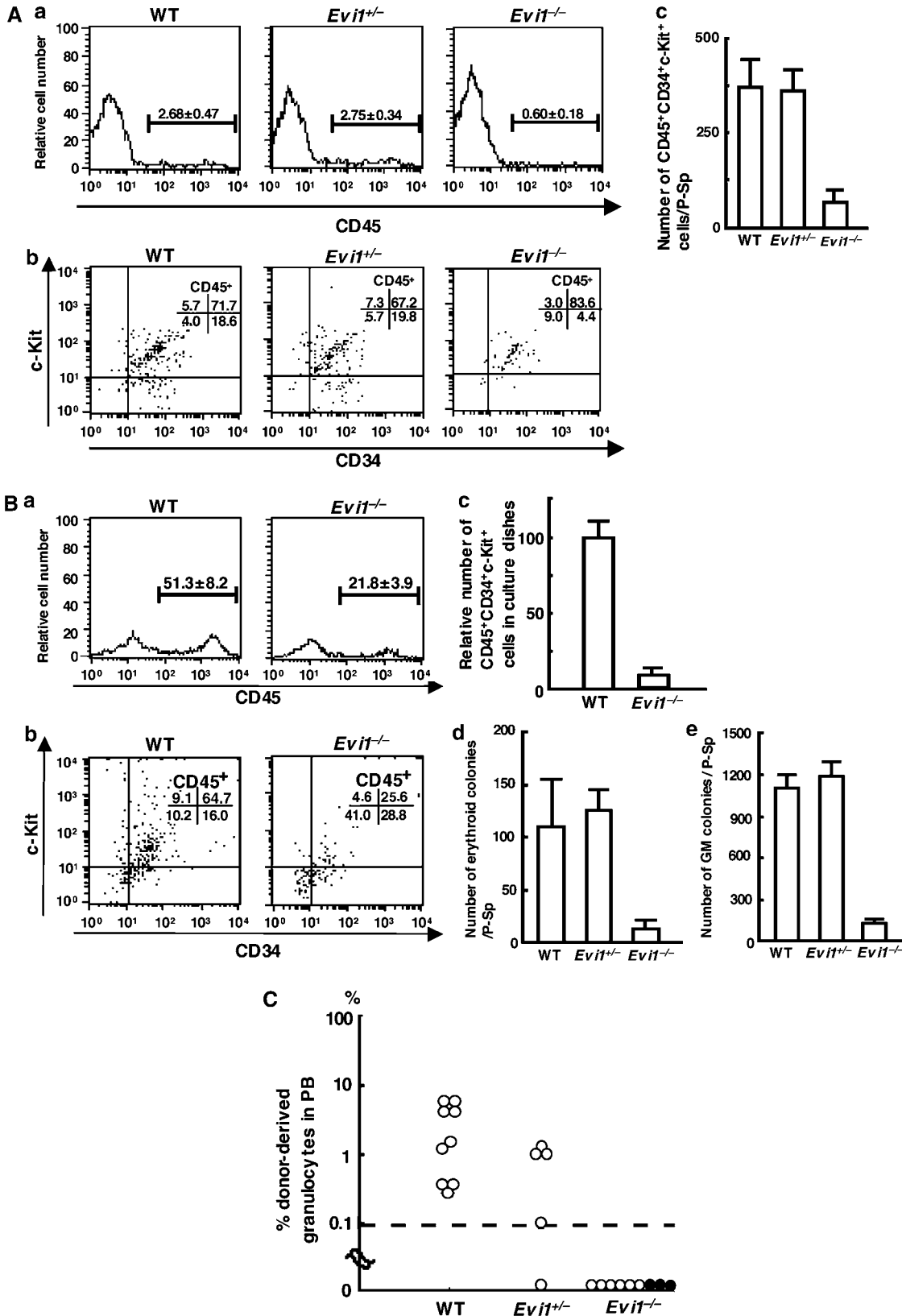


Figure 1 Expression pattern of *Evi1* in hematopoietic cells and gross appearance of E9.5 *Evi1*^{-/-} embryos. (A) Quantitative RT-PCR analysis of *Evi1* mRNA in hematopoietic cells from mouse embryos and adult bone marrow. The embryonic cells analyzed are CD45⁻Ter119⁺ primitive erythrocytes, CD45⁺Ter119⁻ hematopoietic cells other than primitive erythrocytes, CD45⁺c-Kit⁻CD34⁻ mature hematopoietic cells, a CD45⁺c-Kit⁺CD34⁺ HSC-enriched population and para-aortic splanchnopleura (P-Sp). The bone marrow cells analyzed are CD4⁺/CD8⁺, T cells; B220⁺, B cells; CD11b⁺, macrophages and monocytes; Gr-1⁺, granulocytes; Ter119⁺, erythrocytes; CD41⁺, megakaryocytes; CD45⁺Lin⁺, mature hematopoietic cells; CD45⁺Lin⁻, immature hematopoietic cells; c-Kit⁺Sca-1⁺Lin⁻, HSC-enriched population. A mixture of anti-Mac-1, -Gr-1, -B220, -CD4, -CD8 and -Ly-6 antibodies was used as a lineage marker (Lin). *Evi1* mRNA was assayed by real-time PCR (Materials and methods). The data were normalized to GAPDH mRNA and calibrated to the *Evi1*/GAPDH ratio (ΔC_t) in CD45⁻Ter119⁺ cells in mouse embryos and CD45⁺Lin⁺ in adult bone marrow. The data are the mean and standard deviation of 2^{- $\Delta\Delta C_t$} in triplicate assays. (B) (a) The yolk sac from *Evi1*^{-/-} embryos shows severe anemia and defective large vessel development, while large vessels developed and were organized in the yolk sac of *Evi1*^{+/-} (b) and wild-type embryos at E9.5 (c). (d-f) Gross appearance of *Evi1*^{-/-} (d), *Evi1*^{+/-} (e) and wild-type (d) embryos at E9.5. The *Evi1*^{-/-} embryo is smaller and much paler than the wild-type littermate, while also showing pericardial effusion and hemorrhaging.

hematopoietic cells were analyzed by fluorescence activated cell sorting (FACS). The majority of CD45⁺ hematopoietic cells recovered from wild-type P-Sp cultures exhibited the CD34⁺c-Kit⁺CD45⁺ HSC phenotype (64.7% in Figure 2Bb).

In contrast, the number of CD34⁺c-Kit⁺CD45⁺ HSCs in the *Evi1*^{-/-} P-Sp cultures was significantly lower (25.6% in CD45⁺ cells) than that obtained in the controls, indicating a failure of expansion and maintenance of HSCs in *Evi1*^{-/-}



P-Sp culture (Figure 2Ba–c). To examine the differentiation capacity of the *Evi1*-deficient hematopoietic cells, hematopoietic cells derived from P-Sp explants were subjected to *in vitro* colony assays in a semisolid agar culture (Iscove *et al*, 1974) supplemented with stem cell factor (SCF), interleukin 3 (IL-3) and erythropoietin (Epo). Cells from the *Evi1*^{-/-} P-Sp culture from each P-Sp region gave rise to 33.3 and 22.1% erythroid and GM colonies, respectively, relative to those from wild-type embryos (Figure 2Bd and e). An analysis of the differentiation markers after P-Sp explants on OP9 cells for 7 days demonstrated that the differentiation capacity of HSCs in *Evi1*^{-/-} mice was not grossly impaired in terms of the erythroid and GM lineages (Supplementary Figure 2). These results again indicated the inefficient expansion of hematopoietic stem and progenitor cells in *Evi1*^{-/-} P-Sp cultures with a differentiation capacity to erythroid and myeloid cells.

Defective activities of hematopoietic stem cells in P-Sp of the *Evi1*^{-/-} embryos

We next investigated long-term repopulation capacity of HSCs in the *Evi1*^{-/-} P-Sp region. Using an irradiated adult mouse as a recipient, the definitive HSC activity was first detectable in the Aorta-Gonad-Mesonephros (AGM) region of the embryo at day 10.5 by the transplantation of donor test cells with competitor cells (Medvinsky and Dzierzak, 1996). Since the *Evi1*^{-/-} embryo died on E10.5, we could not use the same strategy. Instead, we transplanted the donor hematopoietic cells from the E9.5 P-Sp region into the livers of sublethally conditioned newborn mice, and this strategy has been reported to detect the HSC activity as early as on day 8 or 9 in both yolk sac and P-Sp (Yoder *et al*, 1997).

One-embryo-equivalent cells from E9.5 P-Sp of *Evi1*^{+/+}, *Evi1*^{+/-} or *Evi1*^{-/-} embryos (Ly5.2⁺) were transplanted into a busulfan-conditioned newborn recipient (Ly5.1⁺). The average number of hematopoietic cells from each P-Sp region was almost the same among the three lineages with over 90% viability (Supplementary Table 1). At 3 months post-transplant, the donor-derived Ly5.2⁺ cells could be detected in the peripheral blood of the recipients that received P-Sp cells from the *Evi1*^{+/+} (2.56% on an average) and *Evi1*^{+/-} (0.62% on an average) but not from the *Evi1*^{-/-} embryos (Figure 2C). Since the number of HSCs from *Evi1*^{-/-} P-Sp at E9.5 was one-fifth of those from wild-type P-Sp (Figure 2A), we further combined and transplanted five-embryo-equivalent cells from P-Sp of *Evi1*^{-/-} into a busulfan-conditioned newborn recipient. But no donor-derived cells could be detected in the peripheral blood of the three recipients until

3 months (Figure 2C, closed circles). As demonstrated above, the differentiation capacity of hematopoietic cells from the *Evi1*^{-/-} P-Sp is not grossly impaired to make GM colonies on OP9 cells *in vitro* (Figure 2Be). However, no differentiated granulocytes derived from the *Evi1*^{-/-} embryo were detected in the recipient mice. Since the GM colony-forming cells are mainly committed macrophage progenitor cells, they do not show the *in vivo* reconstitution activity for any lineages, including granulocytes. Thus, *Evi1* is essential for the long-term repopulation capacity of HSCs, which is impaired in an *Evi1* dose-dependent manner in *Evi1*^{+/-} and *Evi1*^{-/-} embryos. Correspondingly, definitive HSC in the yolk sac from *Evi1*^{-/-} embryos (E9.5) did not contribute to reconstitution at all in the conditioned newborn recipients (Supplementary Figure 3).

Defects of *Evi1*^{-/-} mutant embryos in vascular remodeling and angiogenesis

With respect to hematopoiesis and angiogenesis, we recently showed that HSCs play an important role in embryonic angiogenesis due to their secretion of an angiogenic factor, angiopoietin-1 (Ang-1) (Takakura *et al*, 2000). Because the number of HSCs significantly decreased in the *Evi1*^{-/-} embryos, we next determined whether the vascular system of the *Evi1*^{-/-} embryos was normally organized. The pattern of the vascular system of the *Evi1*^{-/-} embryo was studied by whole mount staining of E9.5 embryos using the anti-PECAM-1 monoclonal antibody, which detects differentiated endothelial cells. In comparison to wild-type embryos (Figure 3Aa and c), we found that whole *Evi1*^{-/-} embryos failed to form an organized vascular network at E9.5 (Figure 3Ab and d). The vascular network of the *Evi1*^{-/-} embryos was generally less complex than that of the wild-type embryos (Figures 3Ac and d). In contrast, the homozygous mutants exhibited plexus-like vascular networks and vessels in the brain periphery, which either did not develop or tended to degenerate, suggesting that gross defects in the vascular branching were observed, especially in the head. Because such embryos have already finished ‘turning’ at that stage, it is suggested that the abnormalities in the vascular system are possibly not caused by the growth retardation of *Evi1*^{-/-} embryos. In particular, extensive remodeling, resulting in the formation of large and small vessels, occurred in the yolk sac of the wild-type embryos (Figure 3Ae). However, although the honeycomb-like vascular plexus appeared to form normally at E8.5 in *Evi1*^{-/-} embryos, it remained largely unchanged across most of the surface of the yolk sac at E9.5

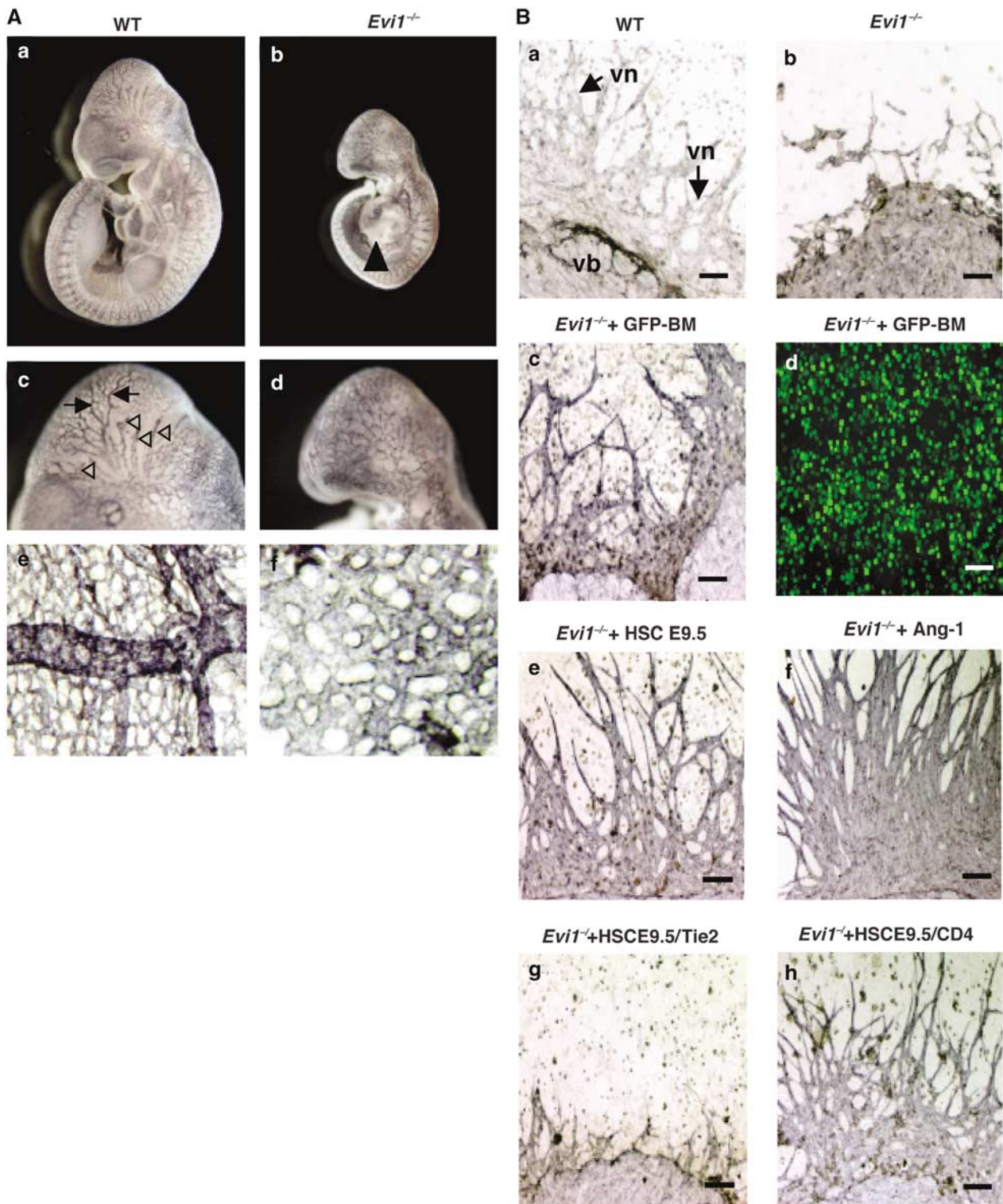
Figure 2 Defects in the *in vitro* proliferation and differentiation of CD45⁺c-Kit⁺CD34⁺ HSCs from E9.5 *Evi1*^{-/-} embryos. **(A)** Incidence of HSCs in E9.5 embryos. The cells from the P-Sp region of E9.5 embryos were stained with anti-CD45, -CD34 and -c-Kit mAbs and analyzed by flow cytometry. (a) CD45⁺ cells were gated (percentages of CD45⁺ cells are indicated in the panel). (b) CD45⁺ cells were examined for the expression of CD34 and c-Kit (percentages of each fraction are indicated in the upper right quadrant). (c) The number of CD45⁺c-Kit⁺CD34⁺ cells in P-Sp from *Evi1*^{-/-}, *Evi1*^{+/-} and wild-type embryos at E9.5 was determined. The columns represent the mean values ± s.d. (*n* = 5). **(B)** *In vitro* hematopoiesis in P-Sp cultures. The cells from the P-Sp cultures on OP9 cells were harvested at 7 days (a–c) and 9 days (d, e) in culture. (a) CD45⁺ cells that developed in culture were gated (the percentages of CD45⁺ cells are indicated in the panel). (b) CD45⁺ cells were examined for the expression of CD34 and c-Kit (the percentages of each fraction are indicated in the upper right quadrant). (c) The numbers of CD45⁺c-Kit⁺CD34⁺ cells in P-Sp culture using *Evi1*^{-/-} and wild-type P-Sp were determined. The columns represent the mean values ± s.d. (*n* = 5). (d, e) The number of progenitor cells that gave rise to erythroid (d) and GM colonies (e) was determined after 7 days of culture. **(C)** *In vivo* hematopoietic reconstitution by transplanted cells. One-embryo-equivalent cells from E9.5 P-Sp were injected into a conditioned newborn recipient (open circle). Five-embryo-equivalent cells from *Evi1*^{-/-} P-Sp were transplanted into a recipient mouse (filled circle). At 8–12 weeks after the transplantation, the proportion of the donor-derived cell population in the recipient granulocytes was determined (%).

(Figure 3Af), suggesting that the remodeling of the vessels did not completely occur in the *Evi1*^{-/-} embryo.

Ang-1 secreted from HSCs prevents defective angiogenesis in P-Sp culture from *Evi1*^{-/-} embryos

To analyze the vascular defects in *Evi1*^{-/-} embryo, we used an *in vitro* P-Sp culture analysis on OP9 cells to determine the *in vitro* differentiation of endothelial cells and vascular network formation (Takakura *et al*, 2000). Explants from

wild-type embryos developed many round cells adhering to the presumptive vascular network area (Figure 3Ba). In contrast, *Evi1*^{-/-} P-Sp explants generated a small number of hematopoietic cells (Figure 3Bb). After immunostaining with anti-PECAM-1 antibody, it was shown that the wild-type explant generated vascular beds (vb) and networks (vn) (Figure 3Ba); on the other hand, poor vascular network formation was observed in the cultures of *Evi1*^{-/-} explants (Figure 3Bb). In proportion to the number of hematopoietic



cells, the area of the vascular network was reduced in culture of *Evi1*^{-/-} explants (Figure 3Bb). Since the network formation is normally promoted by Ang-1 secreted from developing HSCs in P-Sp cultures (Takakura *et al*, 2000), the defects in the development and proliferation of HSCs in *Evi1*^{-/-} P-Sp cultures have been suggested to possibly be one of the reasons for the failure in vascular remodeling.

To test the hypothesis that hematopoietic cells could promote angiogenesis in *Evi1*^{-/-} P-Sp cultures, HSCs from the adult bone marrow of transgenic mice harboring green fluorescent protein (GFP) (Okabe *et al*, 1997) were sorted by flow cytometry and then added to a P-Sp culture of *Evi1*^{-/-} embryos. As shown in Figure 3Bc, a fine vascular network stained by anti-PECAM-1 antibody was developed and coincided with the region where HSCs formed a colony. Under fluorescence microscopy, all GFP-positive cells demonstrated a round shape (Figure 3Bd), suggesting that exogenous adult HSCs did not differentiate into elongated endothelial cells. Moreover, the addition of CD45⁺c-Kit⁺CD34⁺ cells from E9.5 wild-type embryos or recombinant Ang-1 (200 ng/ml) to *Evi1*^{-/-} P-Sp cultures also promoted the vascular network (Figure 3Be and f). Next, to determine whether Ang-1 secreted from HSCs could restore the defective angiogenesis in *Evi1*^{-/-} embryos, we added HSCs from E9.5 wild type either with the recombinant Tie2-Fc fusion protein, which contains the Tie2 ectodomain and thereby acts as an inhibitor by sequestering Ang-1, or with recombinant CD4-Fc as a control to *Evi1*^{-/-} P-Sp cultures. The vascular networks were restored by HSCs with CD4-Fc (Figure 3Bh), but they were not restored by addition of HSCs with Tie2-Fc (Figure 3Bg), suggesting that the defective angiogenesis in *Evi1*^{-/-} embryos is possibly related to a defect in HSCs due to the production of Ang-1.

Decreased expression of Tie2/angiopoietin signaling molecules and GATA gene family in the *Evi1*^{-/-} P-Sp region

Next, expression of regulator molecules in angiogenesis at the *Evi1*^{-/-} P-Sp region was examined by quantitative RT-PCR. The expression of *Ang-1*, *Ang-2* and *Tie2* in P-Sp from *Evi1*^{-/-} embryos decreased markedly, while the expression of vascular endothelial growth factor receptor (*VEGFR*)-1 and *VEGFR*-2 did not significantly change (Figure 4), suggesting that loss of angiopoietin signaling likely causes the defects in vascular remodeling seen in *Evi1*^{-/-} embryos (Figure 3B). On the other hand, it was reported that the angiopoietin signaling is not required for the differentiation and proliferation of

embryonic and fetal hematopoiesis (Puri and Bernstein, 2003). Since *GATA-2* is essential for the proliferation and maintenance of HSCs and hematopoietic progenitors (Tsai

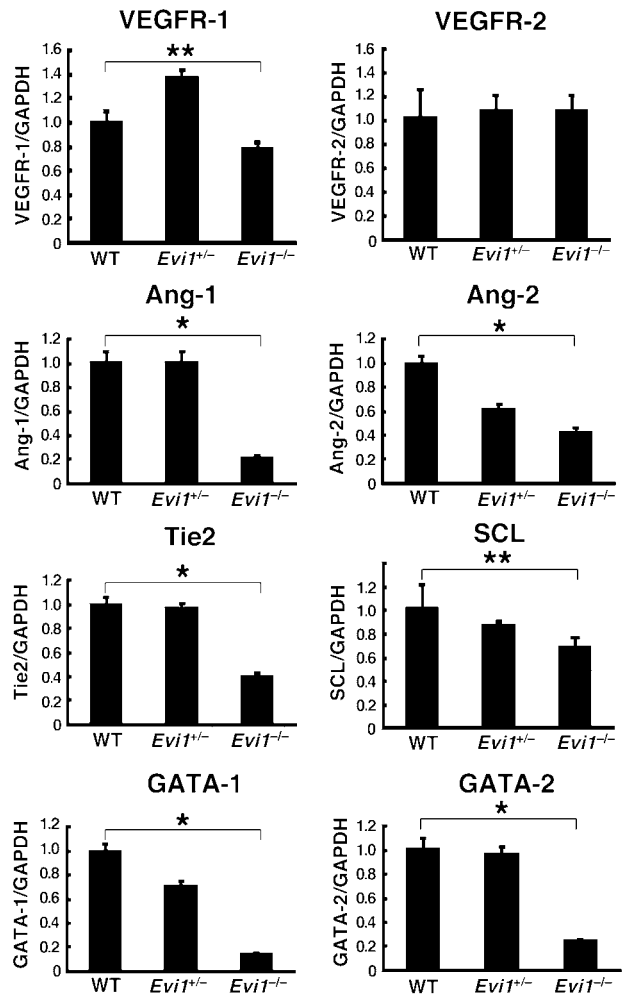


Figure 4 Decreased expression of angiopoietin signaling molecules and GATA gene family in the *Evi1*^{-/-} P-Sp region. An analysis of mRNA expression of several genes related to hematopoiesis or angiogenesis in P-Sp from *Evi1*^{-/-}, *Evi1*^{+/-} and the wild-type embryos at E9.5 by quantitative RT-PCR. The mRNA expression of each gene was normalized to that of GAPDH mRNA and calibrated to the gene/GAPDH ratio (ACT) in wild-type embryos. The relative expression rate in each gene is presented as the mean and standard deviation of 2^{-ΔΔCt} in quadruplicate assays. **P*<0.001; ***P*<0.01, relative to controls.

Figure 3 Defects in vascular remodeling and network formation in E9.5 *Evi1*^{-/-} embryos. (A) Whole-mount PECAM-1-stained wild-type (a) and *Evi1*^{-/-} (b) embryos at E9.5. Panels (c) and (d) are high-power views of panels (a) and (b), respectively. The *Evi1*^{-/-} embryo shows pericardial effusion (arrowhead in (b)). The arrows and arrowheads in (c) indicate the remodeled and organized arteries (arrows) and venous vessels (arrowheads). Highly branched small capillaries and network forming vessels were observed in wild type. *Evi1*^{-/-} counterparts in (d) show no remodeled and organized arteries or veins, and a smaller caliber change in the vessels. (e, f) Yolk sac vascularization. Highly branched small capillaries were evident in wild type (e), while no remodeled or caliber changed vessel was observed in the yolk sac of *Evi1*^{-/-} (f). (B) Requirement of HSC development for angiogenesis *in vitro*. P-Sp explants from *Evi1*^{-/-} (a) and wild-type (b) embryos were dissected at E9.5 and cultured on OP9 cells. P-Sp cultures were stained with anti-PECAM-1 mAbs. The number of hematopoietic cells (round cells) in *Evi1*^{-/-} P-Sp cultures (*Evi1*^{-/-}) (b) was significantly less than that observed in wild-type (WT) cultures (a). Defects in the vascular network (vn) *in vitro* are evident in *Evi1*^{-/-} P-Sp cultures (b) in comparison to WT cultures (arrows in (a)). The bar indicates 0.1 mm. (c) Development of vascular network stained with anti-PECAM-1 mAbs in *Evi1*^{-/-} P-Sp culture with HSCs enriched from GFP-positive adult bone marrow (*Evi1*^{-/-} + GFP-BM). (d) Detection of GFP-positive cells by fluorescence microscopy in (c). The development of vascular network in *Evi1*^{-/-} P-Sp culture with HSCs from E9.5 WT embryos (*Evi1*^{-/-} + HSC E9.5) (e) or with the addition of 200 ng/ml recombinant Ang-1 (*Evi1*^{-/-} + Ang-1). (f) Recombinant Tie2-Fc fusion protein was added with HSCs from E9.5 WT embryos and inhibited the endothelial cell growth of *Evi1*^{-/-} cells by HSC (*Evi1*^{-/-} + HSC E9.5/Tie2-Fc). (g) Recombinant CD4-Fc fusion protein was added with HSC and did not inhibit the effect by HSC as a control HSC (*Evi1*^{-/-} + HSC E9.5/CD4-Fc) (h). The bar indicates 0.1 mm.

et al, 1994), and *GATA-1* plays a role in the differentiation of hematopoietic cells, the expression of *GATA-1* and *GATA-2* was determined and it was found to markedly decrease in the P-Sp region of the *Evi1*^{-/-} embryos (Figure 4). In contrast, the expression of *SCL*, which is essential for the development of definitive HSCs, did not significantly change, suggesting that the decreased expression of *GATA-1* or/and *GATA-2* is probably related to the defective HSC activity in the *Evi1*^{-/-} embryo.

In vitro prevention of defective proliferation of Evi1^{-/-} HSCs via GATA-2

To further support the hypothesis that *Evi1* plays a role in regulating the expression of *GATA-1* or *GATA-2*, we examined whether the *Evi1* expression prevents a decreased expression of *GATA* family in *Evi1*^{-/-} P-Sp. P-Sp explants alone were infected with either an *Evi1* retrovirus (*Evi1*-IRES-EGFP) or a mock EGFP retrovirus (EGFP) as a control (Kaneko *et al*, 2001) and were then collected for a quantitative RT-PCR analysis on day 4. A two-fold increase in the expression level of *GATA-2* mRNA was detected in *Evi1*^{-/-} P-Sp infected with *Evi1* retrovirus (Figure 5A), while the *GATA-2* mRNA levels remained lower in *Evi1*^{-/-} P-Sp infected with control EGFP virus. There were no alterations in the expression levels of GFP among P-Sp explants, which were all infected with either *Evi1* or EGFP alone (Supplementary Figure 4A). Along with the *GATA-2* expression, the expression of *Tie2* and *GATA-1* was upregulated by the *Evi1* expression, but the expression of *Ang-1* and *Ang-2* did not significantly change (Figure 5A).

Moreover, we examined whether the enforced expression of *Evi1*, *GATA-1* or *GATA-2* enables the proliferative capacity of HSCs derived from *Evi1*^{-/-} embryos *in vitro* to return to its original level. P-Sp explants on OP9 cells were infected with *Evi1*, *GATA-1*, *GATA-2* or a mock (EGFP) retrovirus as a control. On day 7 of culture, the cells were subjected to FACS analysis and the number of CD45⁺c-Kit⁺CD34⁺ cells was counted. Many GFP⁺ cells were generated from *Evi1*^{-/-} P-Sp infected with the *Evi1* (+*Evi1*) or the *GATA-2* retrovirus (+*GATA-2*) and most of them were CD45⁺c-Kit⁺CD34⁺ cells (Supplementary Figure 4B). On the other hand, only a few GFP⁺CD45⁺c-Kit⁺CD34⁺ cells were generated from *Evi1*^{-/-} P-Sp infected with the GFP retrovirus (+GFP). As shown in Figure 5B, the *Evi1* or *GATA-2* expression, but not that of *GATA-1*, in *Evi1*^{-/-} P-Sp was able to increase the number of CD45⁺c-Kit⁺CD34⁺ cells up to that of wild-type P-Sp. Therefore, these results showed that the enforced expression of *Evi1* or *GATA-2* helps to maintain the proliferative capacity of HSCs and/or early hematopoietic progenitors in *Evi1*^{-/-} embryos. Taken together, these data suggested that *Evi1* plays a crucial role in both maintaining and proliferating HSCs in the P-Sp region by upregulating *GATA-2* expression.

Reduced expression of GATA-2 in each HSC from Evi1^{-/-} mutant embryos

To determine whether *Evi1* plays a role in regulating the expression of *GATA-2* *in vivo*, we assayed the expression of the GFP reporter driven by the *GATA-2* 7.0IS promoter (kindly provided by Dr Masayuki Yamamoto, Tsukuba University, Japan) in *Evi1*^{-/-} embryos. The murine *GATA-2* gene utilizes two different first exons. The distal IS exon is specifically used in hematopoietic and neural cells, whereas the proximal IG exon is used in a variety of cells (Minegishi *et al*, 1998). In

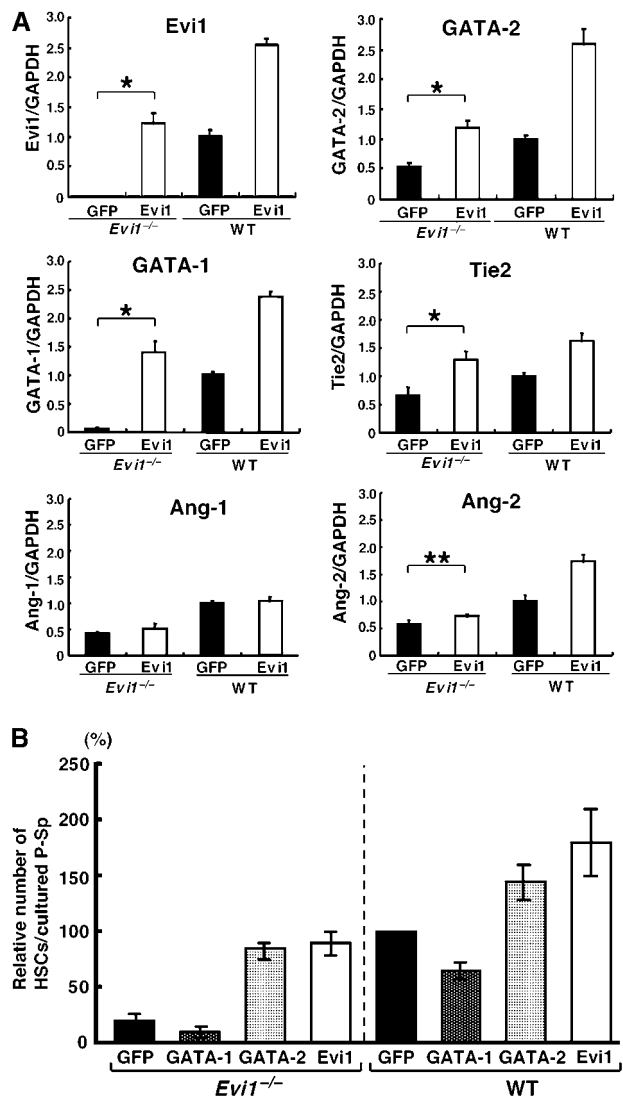
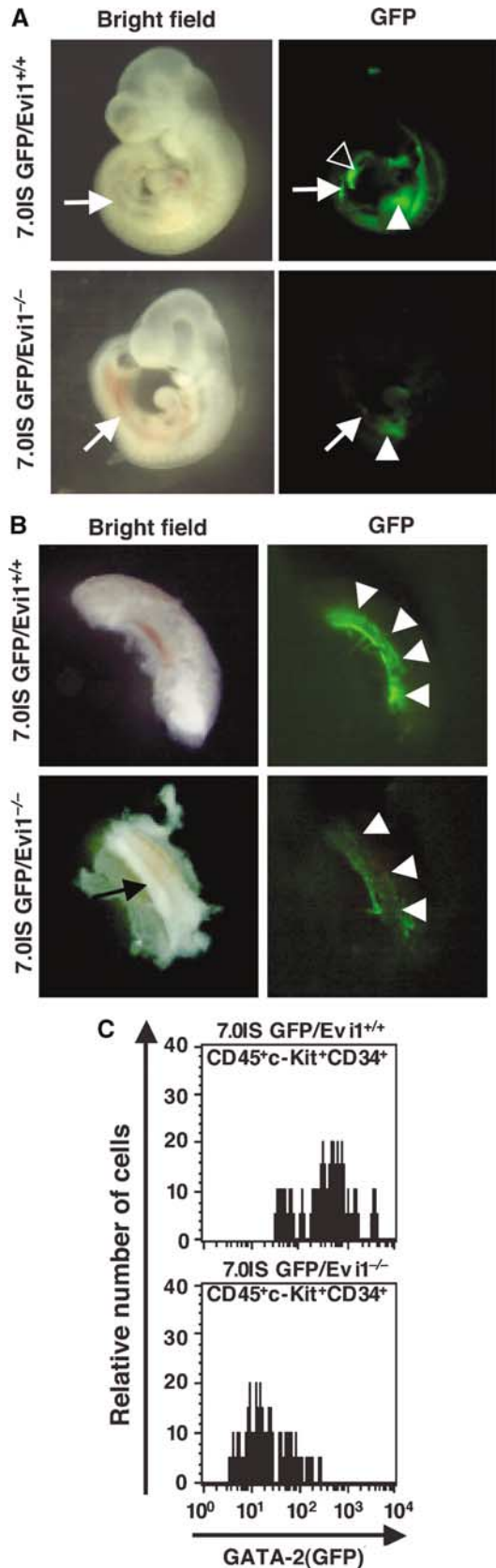


Figure 5 Prevention of defective hematopoiesis in *Evi1*^{-/-} P-Sp cultures by *GATA-2*. (A) *Evi1* maintains the expression of *GATA-2* mRNA in E9.5 *Evi1*^{-/-} P-Sp. P-Sp explants from both *Evi1*^{-/-} (*Evi1*^{-/-}) and wild-type (WT) E9.5 embryos were infected with either an *Evi1* retrovirus (*Evi1*; open square) or a mock EGFP retrovirus (GFP; closed square) as a control. The cells from P-Sp cultures were harvested at 4 days in culture. The mRNA expression of each gene was assayed by quantitative RT-PCR, and then it was normalized to that of GAPDH mRNA and calibrated to the gene/GAPDH ratio (Δ CT) in wild-type P-Sp cells using a control expression vector (EGFP). The relative expression rate in each gene is presented as the mean and standard deviation of 2^{- Δ ACT} in quadruplicate assays. **P* < 0.001; ***P* < 0.01, relative to controls. (B) P-Sp explants (*Evi1*^{-/-} or WT) on OP9 cells were infected with *GATA-1* (*GATA-1*), *GATA-2* (*GATA-2*), *Evi1* (*Evi1*) or a mock EGFP (GFP) retrovirus as a control. The columns represent the ratio of the number of CD45⁺c-Kit⁺CD34⁺ cells in P-Sp cultures relative to those in the wild-type P-Sp cultures infected with a mock EGFP retrovirus (100%). Three independent experiments were performed.

transgenic mice containing the 7.0ISGFP construct, which includes the 7.0 kb 5' flanking region of the *GATA-2* IS exon, the GFP expression shows the endogenous expression profile of *GATA-2* in hematopoietic and neural cells (Minegishi *et al*, 1999). These mice enabled us to analyze the expression of *GATA-2* *in vivo*. GFP-positive cells were easily detected in P-Sp, liver rudiment and the vitelline artery (VA) in 7.0IS-GFP/

Evi1^{+/+} mouse embryos, while the 7.0IS-GFP/*Evi1*^{-/-} mouse embryos showed a markedly decreased number of GFP-positive cells (Figure 6A and B). Moreover, the intensity of GFP significantly decreased in each sorted CD45⁺

c-kit⁺CD34⁺ cell in P-Sp from 7.0IS-GFP/*Evi1*^{-/-} embryos in comparison to that from 7.0IS-GFP/*Evi1*^{+/+} embryos (Figure 6C), suggesting that the *GATA-2* expression was selectively impaired in each purified CD45⁺c-Kit⁺CD34⁺ cell in P-Sp of *Evi1*^{-/-} mice. These findings strongly support the hypothesis that *Evi1* plays a role in the transcriptional regulation of *GATA-2* in HSCs.



Regulation of *Evi1* in activation of the *GATA-2* IS promoter

To determine whether *Evi1* directly regulates the transcription of *GATA-2*, we first searched for the DNA-binding sequences of *GATA-2* in the 7.0 kb 5' promoter region of the *GATA-2* IS exon, which is necessary for the endogenous expression of *GATA-2* in hematopoietic and neural cells (Minegishi *et al*, 1998, 1999). *Evi1* protein contains two independent DNA-binding domains, 1 and 2 (D1 and D2), with seven and three zinc-finger repeats, respectively. Each domain binds to a different consensus sequence, similar to the GATA sequences in the case of D1 (D1-CONS: [GAC/TA] N₀₋₆ [GAT/CA]) and the ETS sequences in the case of D2 (D2-CONS: GAAGAT or GATGAG) (Morishita *et al*, 1995). We found four possible binding sequences for D1 (Supplementary Figure 5A and Supplementary Table 2A) and eight for D2 (Supplementary Figure 5D and Supplementary Table 2B) in the *GATA-2* IS promoter region. To examine the DNA-binding capacity *in vitro*, each GST-fused DNA-binding domain for *Evi1* (*Evi1*-D1 or *Evi1*-D2) was used in an electrophoretic mobility shift assay (EMSA) (Morishita *et al*, 1995). Among the four possible binding sites for D1, only one site (GACATGGACA, b in Figure 6A) could bind to *Evi1*-D1 and it showed a similar binding affinity for the original D1-CONS (Supplementary Figure 5A). On the other hand, five of eight possible binding sites for D2 (Figure 7A) could bind to *Evi1*-D2 with the same binding affinity for the original D2-CONS (Supplementary Figure 2E and F).

We next examined whether *Evi1* could regulate the transcription of *GATA-2* through direct binding to the binding sequence b for D1 (D1-b) or five other binding sequences for D2 (D2-f, -g, -h, -j and -l) (Figure 7A) using hematopoietic cell lines. Various genomic fragments of the *GATA-2* IS promoter

Figure 6 Loss of *GATA-2* mRNA in P-Sp of E9.5 *Evi1*^{-/-} embryos. The decreased transcription of *GATA-2* in E9.5 *Evi1*^{-/-} embryos. The expression of the transgene driven by the *GATA-2* 7.0IS promoter was analyzed in *Evi1*^{-/-} embryos. 7.0IS-GFP transgenic mice were mated with *Evi1*^{+/+} mice to create 7.0IS-GFP/*Evi1*^{+/+} transgenic mice. After the crossing of 7.0IS-GFP/*Evi1*^{+/+} transgenic mice and *Evi1*^{-/-} mice, the GFP expression in 7.0IS-GFP/*Evi1*^{-/-} transgenic mice was compared to that seen in 7.0IS-GFP/*Evi1*^{+/+} transgenic mice. (A) *GATA-2*-GFP-positive cells were observed in P-Sp (arrow), liver rudiment (arrowhead), the vitelline artery (VA, open arrow) and the dorsal artery (DA) in 7.0IS-GFP/*Evi1*^{+/+} transgenic mice (upper panel), while the frequency of *GATA-2*-GFP-positive cells was markedly decreased in the 7.0IS-GFP/*Evi1*^{-/-} transgenic mice (lower panels). (B) Higher magnification of lower trunk region, which includes P-Sp of 7.0IS-GFP/*Evi1*^{+/+} transgenic mice (upper panel) and 7.0IS-GFP/*Evi1*^{-/-} transgenic mice (lower panels). The arrowheads indicate the P-Sp region. Few GFP⁺ cells were detected in the P-Sp of 7.0IS-GFP/*Evi1*^{-/-} transgenic mice. (C) GFP fluorescence intensity. Histograms of the GFP-positive cells for the CD45⁺c-Kit⁺CD34⁺ cell populations, which are included in P-Sp of 7.0IS-GFP/*Evi1*^{+/+} transgenic mice (upper panel) and 7.0IS-GFP/*Evi1*^{-/-} transgenic mice (lower panels). The data are representative of three independent experiments.

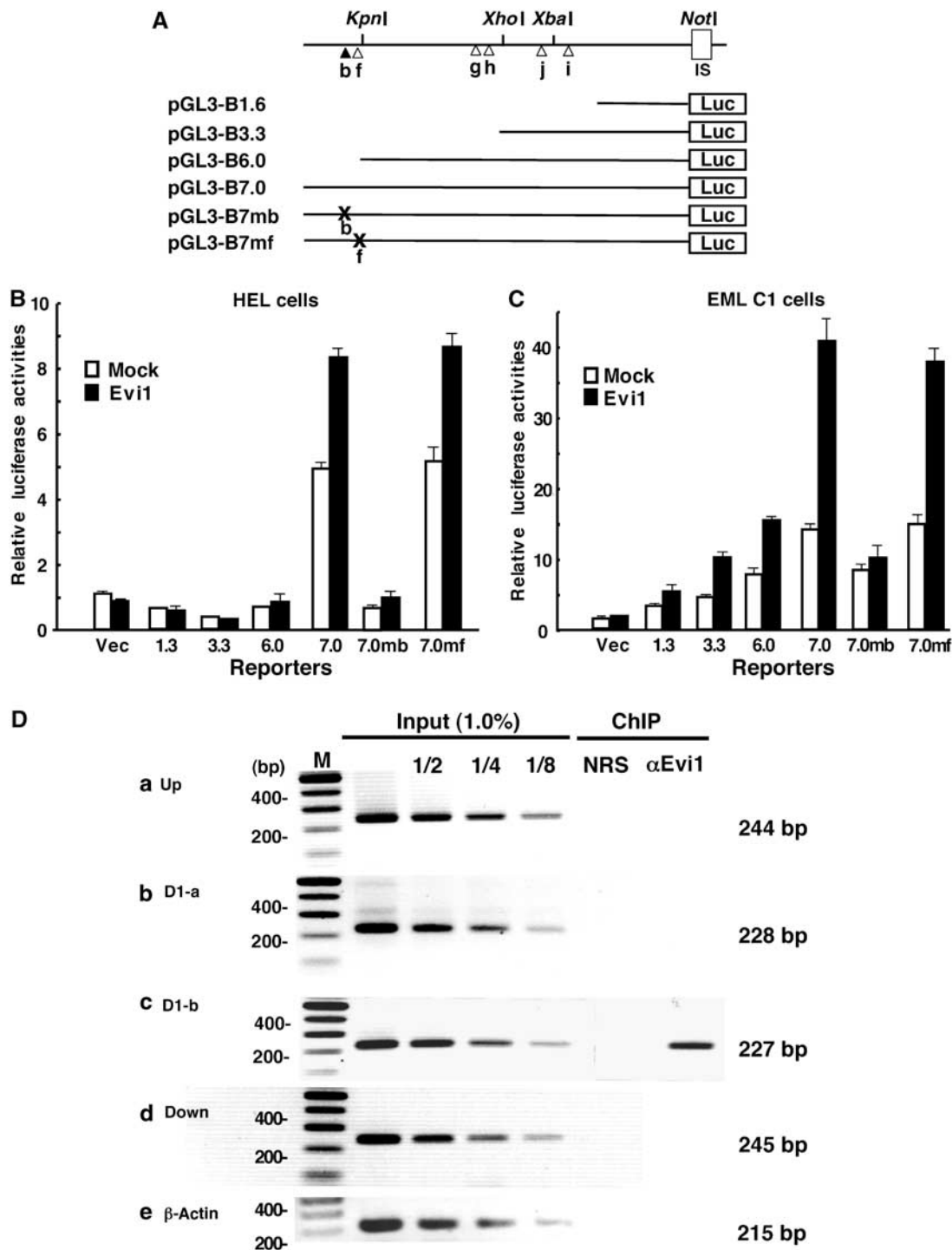


Figure 7 *Evi1* directly binds to the promoter region of *GATA-2* and thus enhances the *GATA-2* transcription. (A) Structure of reporter plasmids of the *GATA-2* promoter region. Various lengths (1.6, 3.3, 6.0 and 7.0 kb) of the promoter region and 7.0 kb of the *GATA-2* promoter region containing mutations in the binding site (b) (from GACATGGACA to GACATGGAGA) (7mb) or in the binding site (f) (from GATGAG to TATGAG) (7mf) were inserted upstream of the luciferase gene in a promoter-less reporter plasmid (pGL3-Basic). The top line shows six possible binding sites (b, f-h, j and l) and four unique restriction sites (*KpnI*, *XhoI*, *XbaI* and *NotI*) located upstream of the IS exon. (B) *GATA-2* promoter activity and transactivation by exogenous *Evi1* in HEL cells. Various *GATA-2* IS promoter-LUC reporter constructs (pGL3-B1.6, 3.3, 6.0 and 7.0) were transfected into HEL cells with (black bar) or without (white bar) an *Evi1* expression vector. A mock vector (pGL3-B) was used as a control (Vec). (C) *GATA-2* promoter activity and transactivation by exogenous *Evi1* in EML C1 cells. The experiment was performed as in HEL cells. (D) Specific DNA binding of *Evi1* to site b detected by ChIP. Five genomic DNA fragments containing each possible DNA-binding site (D1-a or D1-b) were amplified from the genomic DNA from fixed EML C1 cells after immunoprecipitation with normal rabbit serum (NRS) or with anti-*Evi1* antibody (α Evi1). The localization of the amplified regions in *GATA-2* promoter is shown in Supplementary Figure 6A. For controls, each genomic region was amplified from purified DNA with the indicated dilutions after formaldehyde fixation and sonication (Input).

region were isolated and inserted upstream of luciferase cDNA (Luc) in the pGL3-Basic vector (Figure 7A). Each reporter plasmid was transiently transfected into EML C1, a murine stem cell factor-dependent multipotent progenitor cell line (Tsai *et al*, 1994), or HEL, a human erythroleukemia cell line (Martin and Papayannopoulou, 1982). *GATA-2* mRNA is highly expressed in both cell lines, while the *Evi1* mRNA level is higher in HEL but relatively low in EML C1 (data not shown). In HEL cells, the luciferase activity was detected only with the pGL3-B7.0 plasmid, suggesting that it was primarily driven by DNA derived from a 1 kb fragment located -7.0 to -6.0 kb upstream of the *GATA-2* IS promoter (Figure 7B). When each reporter plasmid was transfected with the *Evi1* expression plasmid, the luciferase activity of pGL3-B7.0 increased from five- to eight-fold. In EML C1 cells, the luciferase activity gradually increased as we used constructs from -1.6 to -7.0 kb 5' of the IS promoter, until reaching a 10-fold maximal activation (Figure 7C). When each reporter plasmid was transfected with the *Evi1* expression plasmid, the luciferase activity with the highest transactivation of 2.5-fold by exogenous *Evi1* was obtained with the pGL3-B7.0 plasmid. In this experiment, the activation of *GATA-2* promoter by the enforced *Evi1* expression was only around two-fold that seen in EML C1 and HEL cells, probably because *Evi1* mRNA is already expressed in both cell lines and/or both cell lines may not have a transcriptional setting similar to that of P-Sp in terms of *GATA-2* gene transcription.

In these experiments, the region between -7.0 and -6.0 kb showed the highest promoter activity in both cell lines and its promoter activity was enhanced by exogenous *Evi1*, suggesting that *Evi1* may bind to the region between -7.0 and -6.0 kb of the *GATA-2* IS promoter. Two possible *Evi1* binding sites, D1-b and D2-f, are located within this region. In order to determine the critical site for the transcriptional regulation of *GATA-2*, we generated a reporter plasmid containing a genomic fragment, 7.0 kb 5' of the IS exon containing a mutated D1-b site (pGL3-B7.0mb) (GACATGGACA to GACATGGAGA) or a mutated D2-f site (pGL3-B7.0mf) (GATGAG to TATGAG). In both cell lines, the luciferase activity of pGL3-B7.0mb decreased to the same level as that of pGL3-B6.0 and exogenous *Evi1* failed to transactivate the promoter, whereas the activity of pGL3-B7.0mf did not change in comparison to that of pGL3-B7.0 (Figure 7B and C). These findings indicate that the D1-b site in the region between -7.0 and -6.0 kb is a critical *cis*-element through which *Evi1* regulates the *GATA-2* promoter activity.

To support the hypothesis that the *GATA-2* gene is a direct target of *Evi1* *in vivo*, we undertook a chromatin immunoprecipitation (ChIP) analysis. After the fixation of EML C1 cells, a sonicated DNA-protein mixture was immunoprecipitated by anti-*Evi1* antibody. The genomic region was amplified by PCR using primers specific for the D1-b site with other four different regions in the upstream region of *GATA-2* (Supplementary Figure 6A). As shown in Figure 7D, a 227 bp band containing the D1-b site (D1-b) was amplified from genomic DNA precipitated by anti-*Evi1* antibody. However, a 244 bp band of 2 kb upstream of the D1-b site (Up), a 228 bp band of the D1-a site (D1-a), a 245 bp band of 2 kb downstream of the D1-b site (Down) and β -actin promoter region (β -actin) used as a control were not amplified from the same DNA. We finally observed that the forced

expression of *Evi1* induced *GATA-2* expression in a hematopoietic cell line, EML C1, along with *GATA-1*, *Ang-1*, *Ang-2* and *Tie2* at 2 months after transfection (Supplementary Figure 6B). Taken together, these results support the possibility that *GATA-2* is one of the direct target genes of *Evi1*.

Discussion

In this study, we showed that *Evi1* is expressed at a high level in definitive hematopoietic stem cells of the P-Sp region detected by quantitative RT-PCR. A detailed analysis of *Evi1* homozygous mutant mice clearly showed a marked reduction in CD45⁺CD34⁺c-Kit⁺ HSCs in the *Evi1*^{-/-} P-Sp region, while also showing defects in the proliferation and maintenance of HSCs in *Evi1*^{-/-} P-Sp cultures *in vitro*. Moreover, *Evi1*^{-/-} P-Sp cells did not exhibit HSCs showing a repopulation capacity.

Among the transcription factors crucial for the development of definitive HSCs in embryos, we showed that the expression of *Evi1* correlates positively with that of *GATA-2* in both the P-Sp region and CD45⁺CD34⁺c-Kit⁺ HSCs. Moreover, the defect in *Evi1*^{-/-} HSCs was most reminiscent of that observed in *GATA-2* homozygous mutant mice (Tsai *et al*, 1994). We found the *GATA-2* expression to significantly decrease in *Evi1*^{-/-} embryos. Through an extensive *GATA-2* promoter analysis *in vitro*, we demonstrated that *Evi1* directly regulates the *GATA-2* transcription by binding to the sequence lying between -6127 and -6108 of the 5' flanking region of the IS (specific) first exon. Furthermore, the constitutive expression of *Evi1* or *GATA-2*, but not *GATA-1*, in *Evi1*^{-/-} P-Sp cells helped to prevent the failure of HSC expansion. These results indicate that *GATA-2* is one of the authentic targets of *Evi1* in HSCs. In *GATA-2* homozygous mutant mice, severe defects in both the yolk sac and definitive hematopoiesis were seen (Tsai *et al*, 1994). On the other hand, yolk sac hematopoiesis appeared intact in *Evi1*^{-/-} embryos, suggesting that a likely differential hierarchical regulation of HSCs exists between the yolk sac and definitive hematopoiesis. Therefore, it is of interest to investigate whether *Evi1* also maintains the long-term repopulating HSCs in bone marrow niche, and to also clarify the authentic targets of *Evi1*, since we herein revealed that *Evi1* mRNA is abundantly and selectively expressed in c-Kit⁺Sca-1⁺Lin⁻ HSCs in adult mouse bone marrow.

We recently showed that HSCs play an important role in angiogenesis during embryogenesis by secreting an angiogenic factor, Ang-1 (Takakura *et al*, 2000). Defects in vascular remodeling are phenotypes commonly seen in mice lacking *SCL*, *Runx1* or *c-Myb*, in which mutant mice show a defective development of definitive HSCs. These mice show embryonic lethality at midgestation with severe hemorrhaging and/or defects in vascular development (Mucenski *et al*, 1991; Okuda *et al*, 1996; Visvader *et al*, 1998). Adding normal HSCs or Ang-1 to P-Sp/OP9 cocultures prevents the defective vascular remodeling in *Runx1* homozygous mutant mice, supporting the role of Ang-1 and HSCs with the secretion of Ang-1 in angiogenesis (Takakura *et al*, 2000). Indeed, the expression of *Ang-1* and its cognate receptor, *Tie2*, significantly decreased in *Evi1*^{-/-} embryos. Taken together with the marked reduction in HSC numbers, the vascular phenotype of *Evi1*^{-/-} embryos could be explained in part by inappropriate Ang-1 signals from HSCs.

Several underlying molecular mechanisms of *Evi1* expression have been proposed, including an enhanced AP-1 activity (Tanaka *et al*, 1994), the antagonizing growth-inhibitory effects of TGF β (Kurokawa *et al*, 1998) and a differentiation block (Morishita *et al*, 1992a; Kreider *et al*, 1993). Since *GATA-2* strongly blocks hematopoietic cell differentiation and stimulates immature cell proliferation (Minegishi *et al*, 2003), it is possible that the ectopic expression of *Evi1* induces an aberrant *GATA-2* expression, which is in some part responsible for the oncogenic activity of *Evi1*. In this respect, it will be interesting to analyze the contribution of *GATA-2* to the leukemic transformation as a downstream target gene of the *Evi1* oncogene.

Materials and methods

Animals

Evi1 mutant mice (Hoyt *et al*, 1997) and 7.0IS-GFP transgenic mice (Minegishi *et al*, 1999) were used in this study. Mice were housed in environmentally controlled rooms of the Laboratory Animal Research Center of Keio University under the guidelines for animal and recombinant DNA experiments of Keio University and of the Research Center for Frontier Bioscience of University of Miyazaki.

In vitro culture of P-Sp

P-Sp explants derived from E9.5 *Evi1*^{-/-}, *Evi1*^{+/-} and wild-type embryos were cultured on a layer of OP9 stromal cells at 37°C in humidified 5% CO₂ air. Maintenance of OP9 cells and P-Sp explant cultures for differentiation to endothelial cells were carried out as described previously (Takakura *et al*, 1998; Oike *et al*, 1999).

Transplantation of P-Sp cells into busulfan-treated neonates

Transplantation of cells into busulfan-treated neonatal mice was performed as described previously (Yoder *et al*, 1997) with a slight modification.

Preparation of cDNA from P-Sp of mice and quantitative RT-PCR analysis

Total RNA was isolated by TRIZOL Reagent (Invitrogen) and 1 μ g of DNase-treated total RNA was reverse transcribed using the Advantage[®] RT-for-PCR Kit (BD Biosciences Clontech). A 10 ng portion of the single-stranded cDNA products was used in each real-time PCR reaction (TaqMan 2 \times Universal PCR Master Mix, PE Applied Biosystems). All samples were normalized to GAPDH mRNA abundance and measured using an ABI Prism 7700 Sequence Detector analyzed by the Sequence Detection System software (version 1.7a) (PE Applied Biosystems).

Retroviral infection of P-Sp

The murine *GATA-1*, *GATA-2* or *Evi1* cDNA was subcloned into a site upstream of an IRES-EGFP construct in the retroviral vector pGCSam (GCSam-GATA-1-IRES-EGFP, GCSam-GATA-2-IRES-EGFP

or GCSam-Evi1-IRES-EGFP) as described previously (Kaneko *et al*, 2001). To produce recombinant retrovirus, plasmid DNA was transfected into 293gp cells along with the VSV-G expression plasmid by CaPO₄ co-precipitation. In expression analysis, P-Sp explants on fibronectin-coated dishes were infected with either an *Evi1* retrovirus (GCSam-Evi1-IRES-EGFP) or a mock retrovirus (GCSam-IRES-EGFP) on days 1 and 3 of culture. On day 4 of culture, cells were collected for RT-PCR analysis, because P-Sp explants could not survive for over 5 days in this culture condition. For *in vitro* P-Sp explants/OP9 stromal cell coculture analysis, P-Sp explants were infected with each retrovirus on days 1 and 3 of culture and were subjected to FACS analysis on day 7.

Production of recombinant Tie2-Fc and CD4-Fc fusion protein

Recombinant fusion proteins of the extracellular domain of murine surface molecules (Tie2 or CD4) and the Fc part of human Ig were designed (Tie2-Fc or CD4-Fc) as described previously (Takakura *et al*, 1998).

Reporter gene assay of the GATA-2 promoter region

A 7 kb fragment with the major transcription initiation site of mouse *GATA-2* (IS exon) was isolated by PCR and four different plasmids for reporter gene assays of the *GATA-2* gene upstream regions (1.6, 3.3, 6.0 and 7.0 kb) were constructed as shown in Figure 7D. Site-directed mutagenesis of the D1-like sequence site (b) and D2-like sequence site (f) was carried out using a QuickChange Site-Directed Mutagenesis Kit (Stratagene).

Chromatin immunoprecipitation analysis

A ChIP analysis was performed as described previously (Weinmann *et al*, 2001). Briefly, EML C1 (1 \times 10⁶) cells were crosslinked with 1% formaldehyde and sonicated. After the chromatin fraction was incubated with anti-Evi1 antibody, immune complexes were bound to protein A Sepharose 4B beads (Amersham) twice. Eluted DNA samples were then analyzed by PCR using specific primer pairs (Supplementary Table 3B) containing 'Up' (2 kb upstream of D1-b), 'Down' (2 kb downstream of D1-b), the D1-like sequence D1-a or D1-b at *GATA-2* promoter region or murine β -actin promoter as shown in Figure 7D. Rabbit polyclonal anti-Evi1 antibody was immunized and made by GST fusion Evi1 protein as described previously (Morishita *et al*, 1995).

Supplementary data

Supplementary data are available at *The EMBO Journal* Online.

Acknowledgements

We thank Dr Schickwann Tsai for providing EML and BHK/MKL cells, Dr Masayuki Yamamoto for providing 7.0IS-GFP transgenic mice and Dr Masafumi Onodera for GCSam-IRES-EGFP. This work was supported by Grants-in-Aid for Scientific Research on Priority Areas and for 21st Century COE program (Life Science) from the Ministry of Education, Culture, Sports, Science and Technology of Japan.

References

- Godin I, Dieterlen-Lievre F, Cumano A (1995) Emergence of multipotent hemopoietic cells in the yolk sac and paraortic splanchnopleura in mouse embryos, beginning at 8.5 days postcoitus. *Proc Natl Acad Sci USA* **92**: 773–777
- Hoyt PR, Bartholomew C, Davis AJ, Yutzey K, Gamer LW, Potter SS, Ihle JN, Mucenski ML (1997) The *Evi1* proto-oncogene is required at midgestation for neural, heart, and paraxial mesenchyme development. *Mech Dev* **65**: 55–70
- Iscoe NN, Sieber F, Winterhalter KH (1974) Erythroid colony formation in cultures of mouse and human bone marrow: analysis of the requirement for erythropoietin by gel filtration and affinity chromatography on agarose-concanavalin. *J Cell Physiol* **83**: 309–320
- Kaneko S, Onodera M, Fujiki Y, Nagasawa T, Nakauchi H (2001) Simplified retroviral vector GCSap with murine stem cell virus long terminal repeat allows high and continued expression of enhanced green fluorescent protein by human hematopoietic progenitors engrafted in nonobese diabetic/severe combined immunodeficient mice. *Hum Gene Ther* **12**: 35–44
- Kreider BL, Orkin SH, Ihle JN (1993) Loss of erythropoietin responsiveness in erythroid progenitors due to expression of the *Evi1* myeloid-transforming gene. *Proc Natl Acad Sci USA* **90**: 6454–6458
- Kurokawa M, Mitani K, Irie K, Matsuyama T, Takahashi T, Chiba S, Yazaki Y, Matsumoto K, Hirai H (1998) The oncoprotein *Evi1* represses TGF-beta signalling by inhibiting Smad3. *Nature* **394**: 92–96
- Martin P, Papayannopoulou T (1982) HEL cells: a new human erythroleukemia cell line with spontaneous and induced globin expression. *Science* **216**: 1233–1235

- Matsugi T, Morishita K, Ihle JN (1990) Identification, nuclear localization, and DNA-binding activity of the zinc finger protein encoded by the *Evi1* myeloid transforming gene. *Mol Cell Biol* **10**: 1259–1264
- Medvinsky AL, Dzierzak EA (1996) Definitive hematopoiesis is autonomously initiated by the AGM region. *Cell* **86**: 897–906
- Minegishi N, Ohta J, Suwabe N, Nakauchi H, Ishihara H, Hayashi N, Yamamoto M (1998) Alternative promoters regulate transcription of the mouse *GATA-2* gene. *J Biol Chem* **273**: 3625–3634
- Minegishi N, Ohta J, Yamagiwa H, Suzuki N, Kawauchi S, Zhou Y, Takahashi S, Hayashi N, Engel JD, Yamamoto M (1999) The mouse *GATA-2* gene is expressed in the para-aortic splanchnopleura and aorta-gonads and mesonephros region. *Blood* **93**: 4196–4207
- Minegishi N, Suzuki N, Yokomizo T, Pan X, Fujimoto T, Takahashi S, Hara T, Miyajima A, Nishikawa S, Yamamoto M (2003) Expression and domain-specific function of *GATA-2* during differentiation of the hematopoietic precursor cells in midgestation mouse embryos. *Blood* **102**: 896–905
- Mitani K, Ogawa S, Tanaka T, Miyoshi H, Kurokawa M, Mano H, Yazaki Y, Ohki M, Hirai H (1994) Generation of the AML1-*EV11* fusion gene in the t(3;21)(q26;q22) causes blastic crisis in chronic myelocytic leukemia. *EMBO J* **13**: 504–510
- Morishita K, Parganas E, Matsugi T, Ihle JN (1992a) Expression of the *Evi1* zinc finger gene in 32Dc13 myeloid cells blocks granulocytic differentiation in response to granulocyte colony-stimulating factor. *Mol Cell Biol* **12**: 183–189
- Morishita K, Parganas E, Parham DM, Matsugi T, Ihle JN (1990) The *Evi1* zinc finger myeloid transforming gene is normally expressed in the kidney and in developing oocytes. *Oncogene* **5**: 1419–1423
- Morishita K, Parganas E, William CL, Whittaker MH, Drabkin H, Oval J, Taetle R, Valentine MB, Ihle JN (1992b) Activation of *EV11* gene expression in human acute myelogenous leukemias by translocations spanning 300–400 kilobases on chromosome band 3q26. *Proc Natl Acad Sci USA* **89**: 3937–3941
- Morishita K, Parker DS, Mucenski ML, Jenkins NA, Copeland NG, Ihle JN (1988) Retroviral activation of a novel gene encoding a zinc finger protein in IL-3-dependent myeloid leukemia cell lines. *Cell* **54**: 831–840
- Morishita K, Suzukawa K, Taki T, Ihle JN, Yokota J (1995) *EV11* zinc finger protein works as a transcriptional activator via binding to a consensus sequence of GACAAGATAAGATAAN_{1–28} CTCATCTTC. *Oncogene* **10**: 1961–1967
- Mucenski ML, McLain K, Kier AB, Swerdlow SH, Schreiner CM, Miller TA, Pietryga DW, Scott Jr WJ, Potter SS (1991) A functional *c-myc* gene is required for normal murine fetal hepatic hematopoiesis. *Cell* **65**: 677–689
- Mucenski ML, Taylor BA, Ihle JN, Hartley JW, Marse III HC, Jenkins NA, Copeland NG (1988) Identification of a common ecotropic viral integration site, *Evi1*, in the DNA of AKXD murine myeloid tumors. *Mol Cell Biol* **8**: 301–308
- Oike Y, Takakura N, Hata A, Kaname T, Akizuki M, Yamaguchi Y, Yasue H, Araki K, Yamamura K, Suda T (1999) Mice homozygous for a truncated form of CREB-binding protein exhibit defects in hematopoiesis and vasculo-angiogenesis. *Blood* **93**: 2771–2779
- Okabe M, Ikawa M, Kominami K, Nakanishi T, Nishimune Y (1997) ‘Green mice’ as a source of ubiquitous green cells. *FEBS Lett* **407**: 313–319
- Okuda T, van Deursen J, Hiebert SW, Grosveld G, Downing JR (1996) AML1, the target of multiple chromosomal translocations in human leukemia, is essential for normal fetal liver hematopoiesis. *Cell* **84**: 321–330
- Park I-K, He Y, Lin F, Laerum OD, Tian Q, Bumgarner R, Klug CA, Li K, Kuhr C, Doyle MJ, Xie T, Schummer M, Sun Y, Goldsmith A, Clarke MF, Weissman IL, Hood L, Li L (2002) Differential gene expression profiling of adult murine hematopoietic stem cells. *Blood* **99**: 488–498
- Perkins AS, Mercer JA, Jenkins NA, Copeland NG (1991) Patterns of *Evi1* expression in embryonic and adult tissues suggest that *Evi1* plays an important regulatory role in mouse development. *Development* **111**: 479–487
- Phillips RL, Ernst RE, Brunk B, Ivanova N, Mahan MA, Deanehan JK, Moore KA, Overton GC, Lemischka IR (2000) The genetic program of hematopoietic stem cells. *Science* **288**: 1635–1640
- Puri MC, Bernstein A (2003) Requirement for the TIE family of receptor tyrosine kinases in adult but not fetal hematopoiesis. *Proc Natl Acad Sci USA* **100**: 12753–12758
- Shimizu S, Nagasawa T, Katoh O, Komatsu N, Yokota J, Morishita K (2002) *Evi1* is expressed in megakaryocyte cell lineage and enhanced expression of *EV11* in UT-7/GM cells induces megakaryocyte differentiation. *Biochem Biophys Res Commun* **292**: 609–616
- Takakura N, Huang XL, Naruse T, Hamaguchi I, Dumont DJ, Yancopoulos GD, Suda T (1998) Critical role of the TIE-2 endothelial cell receptor in the development of definitive hematopoiesis. *Immunity* **9**: 677–686
- Takakura N, Watanabe T, Suenobu S, Yamada Y, Noda T, Ito Y, Satake M, Suda T (2000) A role for hematopoietic stem cells in promoting angiogenesis. *Cell* **102**: 199–209
- Tanaka T, Nishida J, Mitani K, Ogawa S, Yazaki Y, Hirai H (1994) *Evi1* raises AP-1 activity and stimulates *c-fos* promoter transactivation with dependence on the second zinc finger domain. *J Biol Chem* **269**: 24020–24026
- Tsai FY, Keller G, Kuo FC, Weiss M, Chen J, Rosenblatt M, Alt FW, Orkin SH (1994) An early haematopoietic defect in mice lacking the transcription factor *GATA-2*. *Nature* **371**: 221–226
- Visvader JE, Fujiwara Y, Orkin SH (1998) Unsuspected role for the T-cell leukemia protein SCL/tal-1 in vascular development. *Genes Dev* **12**: 473–479
- Weinmann AS, Bartley SM, Zhang T, Zhang MO, Farnham PJ (2001) Use of chromatin immunoprecipitation to clone novel E2F target promoters. *Mol Cell Biol* **21**: 6820–6832
- Yoder MC, Hiatt K, Dutt P, Mukherjee P, Bodine DM, Orlic D (1997) Characterization of definitive lymphohematopoietic stem cells in the day 9 murine yolk sac. *Immunity* **7**: 335–344